

Photochemical Organic Oxidations and Dechlorinations with a  $\mu$ -Oxo Bridged Heme/Non-Heme Diiron Complex

Ian M. Wasser, H. Christopher Fry, Paul G. Hoertz, Gerald J. Meyer,\* and Kenneth D. Karlin\*

Department of Chemistry, Johns Hopkins University, Charles and 34th Streets, Baltimore, Maryland 21218

Received July 9, 2004

Steady state and laser flash photolysis studies of the heme/non-heme  $\mu$ -oxo diiron complex  $[(^6\text{L})\text{Fe}^{\text{III}}-\text{O}-\text{Fe}^{\text{III}}-\text{Cl}]^+$  (**1**) have been undertaken. The anaerobic photolysis of benzene solutions of **1** did not result in the buildup of any photoproduct. However, the addition of excess triphenylphosphine resulted in the quantitative photoreduction of **1** to  $[(^6\text{L})\text{Fe}^{\text{II}}\cdots\text{Fe}^{\text{II}}-\text{Cl}]^+$  (**2**), with concomitant production by oxo-transfer of 1 equiv of triphenylphosphine oxide. Under aerobic conditions and excess triphenylphosphine, the reaction produces multiple turnovers ( $\sim 28$ ) before the diiron complex is degraded. The anaerobic photolysis of tetrahydrofuran (THF) or toluene solutions of **1** likewise results in the buildup of **2**. The oxidation products from these reactions included  $\gamma$ -butyrolactone ( $\sim 15\%$ ) for the reaction in THF and benzaldehyde ( $\sim 23\%$ ) from the reaction in toluene. In either case, the O-atom which is incorporated into the carbonyl product is derived from dioxygen present under workup or under aerobic photolysis conditions. Transient absorption measurements of low-temperature THF solutions of **1** revealed the presence of an (P)Fe<sup>II</sup>-like {P = tetraaryl porphyrinate dianion} species suggesting that the reactive species is a formal (heme)-Fe<sup>II</sup>/Fe<sup>IV</sup>=O(non-heme) pair. The non-heme Fe<sup>IV</sup>=O is thus most likely responsible for C–H bond cleavage and subsequent radical chemistry. The photolysis of **1** in chlorobenzene or 1,2-dichlorobenzene resulted in C–Cl cleavage reactions and the formation of  $\{[(^6\text{L})\text{Fe}^{\text{III}}-\text{Cl}\cdots\text{Fe}^{\text{III}}-\text{Cl}]_2\text{O}\}^{2+}$  (**3**), with chloride ligands that are derived from solvent dehalogenation chemistry. The resulting organic products are biphenyl trichlorides or biphenyl monochlorides, derived from dichlorobenzene and chlorobenzene, respectively. Similarly, product **3** is obtained by the photolysis of benzene–benzyl chloride solutions of **1**; the organic product is benzaldehyde ( $\sim 70\%$ ). A brief discussion of the dehalogenation chemistry, along with relevant environmental perspectives, is included.

## Introduction

Synthetic heme compounds with photolabile axial ligands are potentially excellent photocatalysts for substrate oxidation using dioxygen.<sup>1–4</sup> In the classical systems involving  $\mu$ -oxo diferric hemes such as  $[(\text{TPP})\text{Fe}]_2\text{O}$  (TPP = dianion of tetraphenylporphyrinate), direct excitation into the O  $\rightarrow$  Fe ligand-to-metal charge transfer (LMCT) band results in the photodisproportionation of a  $\mu$ -oxo bridged Fe<sup>III</sup>–O–Fe<sup>III</sup> cofacial porphyrin sandwich into both Fe(II) and Fe(IV)=O

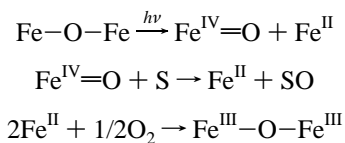
porphyrin monomers.<sup>1–3</sup> The highly reactive porphyrin oxo–ferryl (e.g., peroxidase compound II)<sup>5,6</sup> is capable of substrate oxidation via oxygen atom transfer (OAT), with the subsequent formation of a ferrous heme. The system becomes catalytic in the presence of dioxygen, as outlined below. Quantum yields are not large, and the major fate for the photogenerated Fe(II) and Fe(IV)=O porphyrin subunits is recombination and charge-transfer to reform the parent  $\mu$ -oxo bridged bisporphyrin. Other related systems of interest, showing similar photochemistry, include (P)Fe<sup>III</sup>–R systems (where R = OH, EtO, etc.) where photolysis generates the corresponding (P)Fe<sup>II</sup> and R<sup>•</sup> species.<sup>4,7</sup>

\* Authors to whom correspondence should be addressed. E-mail: karlin@jhu.edu (K.D.K.); meyer@jhu.edu (G.J.M.).

- (1) Richman, R. M.; Peterson, M. W. *J. Am. Chem. Soc.* **1982**, *104*, 5795–5796.
- (2) Peterson, M. W.; Rivers, D. S.; Richman, R. M. *J. Am. Chem. Soc.* **1985**, *107*, 2907–2915.
- (3) Hodgkiss, J. M.; Chang, C. J.; Pistorio, B. J.; Nocera, D. G. *Inorg. Chem.* **2003**, *42*, 8270–8277.
- (4) Maldotti, A.; Molinari, A.; Amadelli, R. *Chem. Rev.* **2002**, *102*, 3811–3836.

- (5) *Cytochrome P450: Structure, Mechanism, and Biochemistry*, 2nd ed.; Ortiz de Montellano, P. R., Ed.; Plenum Press: New York, 1995.
- (6) Sono, M.; Roach, M. P.; Coulter, E. D.; Dawson, J. H. *Chem. Rev.* **1996**, *96*, 2841–2887.
- (7) Maldotti, A.; Bartocci, C.; Varani, G.; Molinari, A.; Battioni, P.; Mansuy, D. *Inorg. Chem.* **1996**, *35*, 1126–1131.

## Catalytic Cycle

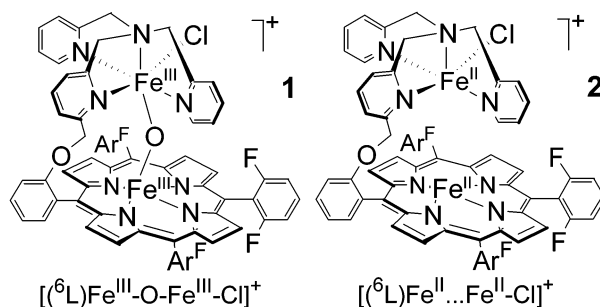


One of our interests lies in the development of model compounds for the active site of nitric oxide reductase (NOR), which has led us to synthesize the heme/non-heme diiron complex  $[(^6\text{L})\text{Fe}^{\text{III}}-\text{O}-\text{Fe}^{\text{III}}-\text{Cl}]^+$  (**1**) (Chart 1).<sup>8</sup> We now report on the photodisproportionation of **1**, the first  $\mu$ -oxo bridged (L)Fe<sup>III</sup>-O-Fe<sup>III</sup>(L') system with nonequivalent iron ligands to be examined in such a manner. The photoreduction of benzene/triphenylphosphine solutions of  $[(^6\text{L})\text{Fe}^{\text{III}}-\text{O}-\text{Fe}^{\text{III}}-\text{Cl}]^+$  (**1**) results in the clean transfer of an oxygen atom to triphenylphosphine, leaving behind the reduction product  $[(^6\text{L})\text{Fe}^{\text{II}}\cdots\text{Fe}^{\text{II}}-\text{Cl}]^+$  (**2**). Similar photo-reactions performed in either tetrahydrofuran or toluene resulted in solvent oxidation. Attempts to perform the photoreduction of **1** in chlorinated solvents resulted in the isolation of  $\{[(^6\text{L})\text{Fe}^{\text{III}}-\text{Cl}\cdots\text{Fe}^{\text{III}}-\text{Cl}]_2\text{O}\}^{2+}$  (**3**), with the additional chlorine atoms in the transition metal complex derived from solvent (or chlorinated substrate) dechlorination. Given the nature of our inequivalent ligand system, it was intriguing to determine whether the heme iron site or the non-heme iron would become a high-valent Fe(IV) ferryl group, as both heme and non-heme oxo-ferryl (i.e., Fe<sup>IV</sup>=O) compounds have been identified.<sup>5,6,9-11</sup> Transient absorption spectroscopy was used to probe the nature of any short-lived intermediate. These experiments suggest the formation of a transient ferrous heme with a high-valent site at the non-heme iron. Taken together, the results suggest that a non-heme iron(IV) oxo moiety is responsible for initiating the observed substrate or solvent oxidation and dechlorination chemistry.

## Experimental Section

**Materials and Methods.** Reagents were obtained in high purity from commercial sources and used as received unless otherwise noted. Tetrahydrofuran (THF) and toluene were purified and dried by passing reagent-grade solvent through a series of two activated alumina columns (Innovative Technology, Newburyport, MA). Benzene was purified and dried by distillation from a sodium/benzophenone ketyl. The deoxygenation of solvents was performed by direct bubbling with argon for 30 min followed by 3 freeze-pump-thaw cycles. Infrared spectra were obtained on a Mattson Galaxy 4030 FT-IR spectrometer. Solid samples were prepared by dissolving a sample in solution in the glovebox, spotting a CaF<sub>2</sub> or NaCl IR window, and allowing the solvent to evaporate. Elemental

Chart 1



analyses were performed by Quantitative Technologies, Inc. (QTI), Whitehouse, NJ. Electrospray ionization mass spectrometry (ESI-MS) was performed at The Ohio State University Chemistry Mass Spectrometry Facility. <sup>1</sup>H NMR spectra were recorded at 300 MHz on a Bruker AMX-300 instrument. Chemical shifts are reported as  $\delta$  values relative to an internal standard (Me<sub>4</sub>Si) and the residual solvent proton peak. The preparation and handling of air-sensitive materials was carried out with Schlenk techniques under argon or in an MBraun Labmaster 130 glovebox under nitrogen.

**Synthesis.**  $[(^6\text{L})\text{Fe}^{\text{III}}-\text{O}-\text{Fe}^{\text{III}}-\text{Cl}]\text{B}(\text{C}_6\text{F}_5)_4$  (**1**) was prepared as described in the literature.<sup>8</sup> The corresponding reduced complex  $[(^6\text{L})\text{Fe}^{\text{II}}\cdots\text{Fe}^{\text{II}}-\text{Cl}]\text{B}(\text{C}_6\text{F}_5)_4$  (**2**) was synthesized by sodium dithionite reduction of **1** according to a literature procedure.<sup>12</sup> The isotope labeled complex  $[(^6\text{L})\text{Fe}^{\text{III}}-^{18}\text{O}-\text{Fe}^{\text{III}}-\text{Cl}]\text{B}(\text{C}_6\text{F}_5)_4$  (**1-<sup>18</sup>O**) was prepared by exposing THF solutions of **2** to <sup>18</sup>O<sub>2</sub>(g). The solvent was removed under reduced pressure and the resulting solid transferred to the glovebox. Subsequent recrystallization from a mixture of THF and heptane, followed by filtration, allowed for the isolation of **1-<sup>18</sup>O**, as determined by FTIR  $\{\nu(\text{Fe}-^{18}\text{O}-\text{Fe}) = 803 \text{ cm}^{-1}; \nu(\text{Fe}^{16}-\text{O}-\text{Fe}) = 844 \text{ cm}^{-1}\}$  spectroscopy and comparison to the known resonance Raman spectroscopic properties of **1-<sup>18</sup>O**.<sup>8</sup>

$\{[(^6\text{L})\text{Fe}^{\text{III}}-\text{Cl}\cdots\text{Fe}^{\text{III}}-\text{Cl}]_2\text{O}\}^{2+}[\text{B}(\text{C}_6\text{F}_5)_4]_2$  (**3**). The bulk photolysis (see Photochemistry subsection, which follows) of a 1,2-dichlorobenzene solution (100 mL) of  $[(^6\text{L})\text{Fe}^{\text{III}}-\text{O}-\text{Fe}^{\text{III}}-\text{Cl}]\text{B}(\text{C}_6\text{F}_5)_4$  (**1**) ( $5 \times 10^{-5}$  M) resulted in the clean formation of **3**, as determined by UV-vis spectroscopy. The air-stable, red complex  $\{[(^6\text{L})\text{Fe}^{\text{III}}-\text{Cl}\cdots\text{Fe}^{\text{III}}-\text{Cl}]_2\text{O}\}^{2+}[\text{B}(\text{C}_6\text{F}_5)_4]_2$  (**3**) was isolated from the crude reaction mixture by removal of the solvent using a high-vacuum rotary evaporator; purification was accomplished by recrystallization from methylene chloride and heptane at -20 °C. Yield: ~80%. <sup>1</sup>H NMR (THF-*d*<sub>8</sub>, 300 MHz):  $\delta$  81 (br, pyrrole-H), 14.13 (m, PY-H), 12.80 (m, PY-H), 7.6-7.18 (*m*- and *p*-phenyl-H), 6.92 (PY-H), 6.83 (PY-H). UV-vis (CH<sub>2</sub>Cl<sub>2</sub>; nm,  $\epsilon \text{ mol}^{-1} \text{ L}^{-1}$ ): 376, 58000; 415, 104000; 507, 13000; 579, 4600; 644, 4500. FTIR (film, cm<sup>-1</sup>) 1647, 1625, 1606, 1583, 1513, 1463, 1372, 1331, 1275, 1236, 1206. ESI-MS: *m/z* 1221  $\{[(^6\text{L})\text{Fe}-\text{Cl}\cdots\text{Fe}-\text{Cl}]^+\}$ . Anal. Calcd for C<sub>174</sub>H<sub>84</sub>B<sub>2</sub>Cl<sub>4</sub>F<sub>52</sub>Fe<sub>4</sub>N<sub>16</sub>O<sub>4</sub> (**3**·2H<sub>2</sub>O): C, 54.23; H, 2.20; N, 5.82. Found: C, 54.23; H, 2.36; N, 5.49.

**Quantum Yield Determination.** The product quantum yields were determined by actinometry as previously described.<sup>13,14</sup> Air-sensitive photoproducts were handled in the glovebox under nitrogen.

**Photochemistry.** Typical experiments involved the preparation of 3 mL of a  $(5-15) \times 10^{-6}$  M solution of  $[(^6\text{L})\text{Fe}^{\text{III}}-\text{O}-\text{Fe}^{\text{III}}-$

(8) Wasser, I. M.; Martens, C. F.; Verani, C. N.; Rentschler, E.; Huang, H.-w.; Moenne-Loccoz, P.; Zakharov, L. N.; Rheingold, A. L.; Karlin, K. D. *Inorg. Chem.* **2004**, *43*, 651-662.

(9) Rohde, J.-U.; In, J. H.; Lim, M. H.; Brennessel, W. W.; Bukowski, M. R.; Stubna, A.; Muenck, E.; Nam, W.; Que, L., Jr. *Science* **2003**, *299*, 1037-1039.

(10) Lim, M. H.; Rohde, J.-U.; Stubna, A.; Bukowski, M. R.; Costas, M.; Ho, R. Y. N.; Munck, E.; Nam, W.; Que, L., Jr. *Proc. Natl. Acad. Sci. U.S.A.* **2003**, *100*, 3665-3670.

(11) Kaizer, J.; Klinker, E. J.; Oh, N. Y.; Rohde, J.-U.; Song, W. J.; Stubna, A.; Kim, J.; Muenck, E.; Nam, W.; Que, L., Jr. *J. Am. Chem. Soc.* **2004**, *126*, 472-473.

(12) Wasser, I. M.; Huang, H.-W.; Moenne-Loccoz, P.; Karlin, K. D. Submitted for publication.

(13) Peterson, M. W.; Richman, R. M. *Inorg. Chem.* **1985**, *24*, 722.

(14) Thompson, D. W.; Kretzer, R. M.; Lebeau, E. L.; Scaltrito, D. V.; Ghiladi, R. A.; Lam, K.-C.; Rheingold, A. L.; Karlin, K. D.; Meyer, G. J. *Inorg. Chem.* **2003**, *42*, 5211-5218.

Cl]B(C<sub>6</sub>F<sub>5</sub>)<sub>4</sub> (**1**) in the glovebox in an appropriate solvent. These solutions were transferred to an airtight four-window quartz cuvette and sealed with either a rubber septum (for aerobic photolyses) or a glass stopper (for anaerobic photolyses). For aerobic photolysis reactions, solutions of [(<sup>6</sup>L)Fe<sup>III</sup>-O-Fe<sup>III</sup>-Cl]B(C<sub>6</sub>F<sub>5</sub>)<sub>4</sub> (**1**) were saturated with dioxygen by direct bubbling of <sup>16</sup>O<sub>2</sub> or <sup>18</sup>O<sub>2</sub> (10 mL) into the prepared solutions using a stainless steel syringe. The pressure of the system was equilibrated to the atmosphere using an attached oil bubbler. Photolyses were carried out in two alternative ways: (1) using a Rayonet photochemical reactor equipped with 350 nm bulbs, with excitation times ranging from 25 min (chlorinated solvents) to 55 min (THF) and 120 min (toluene and benzene/triphenylphosphine) or 24 h (for overnight photobleach experiments); and (2) excitation with 355 nm laser pulses (10–60 mJ cm<sup>-2</sup>) from a Nd:YAG laser (Continuum Surelite II or III) with reaction times ranging from 5 min (chlorinated solvents) to 20 min (THF) and 60 min (toluene and benzene/triphenylphosphine). The photolysis of benzene solutions of [(<sup>6</sup>L)Fe<sup>III</sup>-O-Fe<sup>III</sup>-Cl]B(C<sub>6</sub>F<sub>5</sub>)<sub>4</sub> (**1**) under either condition 1 or 2 resulted in no observed photochemistry. Bulk photolysis reactions in 1,2-dichlorobenzene were performed over the course of 4 days using the Rayonet photochemical reactor and a 100 mL solution of [(<sup>6</sup>L)Fe<sup>III</sup>-O-Fe<sup>III</sup>-Cl]B(C<sub>6</sub>F<sub>5</sub>)<sub>4</sub> (**1**) (1 ~ 5 × 10<sup>-5</sup> M) in a glass reaction tube. The reaction apparatus was gently agitated at periodic intervals. The course of the bulk reaction was monitored by sampling aliquots of the reaction mixture and examining them by UV-vis spectroscopy.

**Transient UV-Vis Laser Flash Photolysis Studies.** Transient absorbance measurements were made using a previously described apparatus.<sup>14</sup> Excitation was accomplished with 355 nm laser pulses (10–30 mJ cm<sup>-2</sup>) from a Nd:YAG laser (Continuum Surelite II or III). The sample was protected from rapid degradation using a fast shutter along with UV and thermal absorbing filter combinations. Samples were prepared in an inert atmosphere glovebox under N<sub>2</sub>, and the four window quartz cuvettes were sealed with a glass stopper. The sample cuvette was held in a cooled methanol jacketed four-window optical dewar held at 198 K. This low temperature assembly has been previously described.<sup>15,16</sup>

**Gas Chromatography-Mass Spectrometry (GC-MS).** Prior to gas chromatographic analysis, photochemical reaction mixtures were exposed to the ambient atmosphere (or bubbled with <sup>18</sup>O<sub>2</sub> (g)) and passed through a short (1 cm) pad of alumina using the reaction medium as eluent. This procedure separated the nonvolatile material derived from [(<sup>6</sup>L)Fe<sup>III</sup>-O-Fe<sup>III</sup>-Cl]B(C<sub>6</sub>F<sub>5</sub>)<sub>4</sub> (**1**) (or derivatives thereof) from the organic reaction products. Reaction products were identified by comparison with retention times of known standards. Quantification was performed by injecting known concentrations of standard to construct a calibration curve. No oxidation products were detected when control experiments were performed in the dark. The GC-MS measurements were made using a AOC-20i autosampler (Shimadzu, 1 μL injections) attached to a Shimadzu QP5050A GC-MS system fitted with a 30 m DB-5MS packed column (J&W Scientific, serial number 0726023).

## Results and Discussion

### Photolysis of [(<sup>6</sup>L)Fe<sup>III</sup>-O-Fe<sup>III</sup>-Cl]<sup>+</sup> (**1**) in Benzene with Triphenylphosphine.

Our initial interest in the photochemistry of [(<sup>6</sup>L)Fe<sup>III</sup>-O-Fe<sup>III</sup>-Cl]B(C<sub>6</sub>F<sub>5</sub>)<sub>4</sub> (**1**) began when we observed an apparent photoreduction of **1** to [(<sup>6</sup>L)Fe<sup>II</sup>...Fe<sup>II</sup>-Cl]B(C<sub>6</sub>F<sub>5</sub>)<sub>4</sub> (**2**) in THF. By contrast, laser flash photolysis or continuous (Rayonet) photolysis (λ<sub>exc</sub> 355 nm) of degassed benzene solutions of [(<sup>6</sup>L)Fe<sup>III</sup>-O-Fe<sup>III</sup>-Cl]B(C<sub>6</sub>F<sub>5</sub>)<sub>4</sub> (**1**) led to no discernible UV-vis spectroscopic changes, even after prolonged (ca. 4 h) photolysis. However, when the reaction was performed in benzene with an excess of triphenylphosphine, we observed the photoreduction (see Supporting Information, Figure S1) of [(<sup>6</sup>L)Fe<sup>III</sup>-O-Fe<sup>III</sup>-Cl]B(C<sub>6</sub>F<sub>5</sub>)<sub>4</sub> (**1**) [λ<sub>max</sub> 418 (Soret), 575 nm] to form the reduced complex [(<sup>6</sup>L)Fe<sup>II</sup>...Fe<sup>II</sup>-Cl]B(C<sub>6</sub>F<sub>5</sub>)<sub>4</sub> (**2**) [λ<sub>max</sub> 415 (Soret), 432 (sh), 532, 550 (sh) nm] with the concomitant formation of a stoichiometric amount of triphenylphosphine oxide (by GC-MS). This reactivity is summarized in Figure 1. It is important to note that excitation into the probable LMCT band (λ ~ 350 nm)<sup>17</sup> of [(<sup>6</sup>L)Fe<sup>III</sup>-O-Fe<sup>III</sup>-Cl]<sup>+</sup> **1** is critical in effecting the photoreduction; the irradiation with either Soret-based excitation at λ<sub>max</sub> 417 nm or Q-band excitation at λ<sub>max</sub> 532 nm resulted in no observed photochemistry.

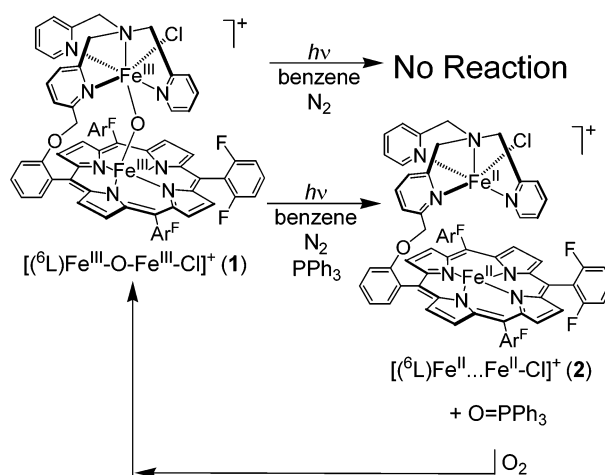


**Figure 1.** Photolysis of [(<sup>6</sup>L)Fe<sup>III</sup>-O-Fe<sup>III</sup>-Cl]<sup>+</sup> (**1**) in benzene results in no observed reaction (top). The photoreduction of [(<sup>6</sup>L)Fe<sup>III</sup>-O-Fe<sup>III</sup>-Cl]<sup>+</sup> (**1**) to [(<sup>6</sup>L)Fe<sup>II</sup>...Fe<sup>II</sup>-Cl]B(C<sub>6</sub>F<sub>5</sub>)<sub>4</sub> (**2**) occurs in benzene/triphenylphosphine solutions, with concomitant oxygenation of triphenylphosphine to triphenylphosphine oxide (bottom). Dioxygen can convert **2** to **1**, explaining the observed photocatalytic PPh<sub>3</sub> oxidation under aerobic conditions.

Since the oxidation of triphenylphosphine to triphenylphosphine oxide is an energetically downhill process, we sought to identify the source of the O-atom that was incorporated into the triphenylphosphine oxide product to rule out auto-oxidation by dioxygen contamination. Anaerobic benzene solutions of [(<sup>6</sup>L)Fe<sup>III</sup>-(<sup>18</sup>O)-Fe<sup>III</sup>-Cl]B(C<sub>6</sub>F<sub>5</sub>)<sub>4</sub> (**1**-<sup>18</sup>O) (see Experimental Section) were photolyzed in the presence of triphenylphosphine. The transfer of an <sup>18</sup>O-atom from **1**-<sup>18</sup>O to triphenylphosphine, thereby forming <sup>18</sup>O=PPh<sub>3</sub>, was confirmed by GC-MS (revealing ~95% <sup>18</sup>O-atom incorporation). Indeed, the formation of triphenylphosphine oxide was not the result of inadvertent dioxygen contamination.

**Aerobic Photolysis.** Solutions of [(<sup>6</sup>L)Fe<sup>III</sup>-O-Fe<sup>III</sup>-Cl]<sup>+</sup> (**1**), prepared in benzene with an excess of triphenylphosphine, were photolyzed in the presence of triphenylphosphine. The transfer of an <sup>18</sup>O-atom from **1**-<sup>18</sup>O to triphenylphosphine, thereby forming <sup>18</sup>O=PPh<sub>3</sub>, was confirmed by GC-MS (revealing ~95% <sup>18</sup>O-atom incorporation). Indeed, the formation of triphenylphosphine oxide was not the result of inadvertent dioxygen contamination.

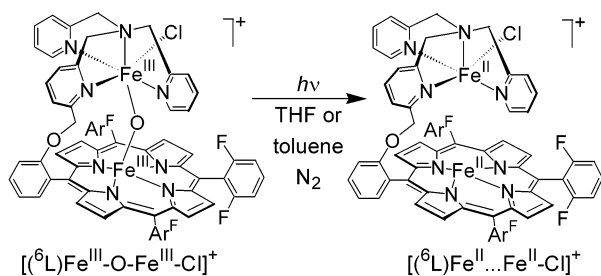
**Aerobic Photolysis.** Solutions of [(<sup>6</sup>L)Fe<sup>III</sup>-O-Fe<sup>III</sup>-Cl]<sup>+</sup> (**1**), prepared in benzene with an excess of triphenylphosphine,

(15) Karlin, K. D.; Haka, M. S.; Cruse, R. W.; Meyer, G. J.; Farooq, A.; Gultneh, Y.; Hayes, J. C.; Zubieta, J. *J. Am. Chem. Soc.* **1988**, *110*, 1196–1207.

(16) Karlin, K. D.; Cruse, R. W.; Gultneh, Y.; Farooq, A.; Hayes, J. C.; Zubieta, J. *J. Am. Chem. Soc.* **1987**, *109*, 2668–2679.

(17) Hendrickson, D. N.; Kinnaird, M. G.; Suslick, K. S. *J. Am. Chem. Soc.* **1987**, *109*, 1243–1244.

Scheme 1



phine, were saturated with dioxygen. Subsequent photolysis reactions, performed for a length of time (ca. 2 h) similar to what had been used in the anaerobic reaction scenario, resulted in the buildup of no observed photoproduct. However, extended photolysis under these conditions (ca. 24 h) resulted in the photobleaching of solutions of  $[(^6L)\text{Fe}^{\text{III}}\text{--O--Fe}^{\text{III}}\text{--Cl}]^+$  (**1**), as observed by the complete loss of all visible color corresponding to the disappearance of the Soret and Q-band absorbances in the resulting UV–vis spectra. An examination of the organic reaction products revealed a modest turnover ( $24 \pm 4$ ) of triphenylphosphine to triphenylphosphine oxide, as determined by GC–MS. However, the bleaching described above suggests extensive oxidative degradation of the heme in **1** (or **2**) has occurred. The apparent catalytic behavior probably results from the facile  $\text{O}_2$ -reoxidation of **2** to **1**, which we have confirmed does occur.<sup>12</sup> The UV–vis spectral identification of **2** was based on observation of the same absorption spectrum upon preparation of benzene solutions of  $[(^6L)\text{Fe}^{\text{II}}\cdots\text{Fe}^{\text{II}}\text{--Cl}]\text{B}(\text{C}_6\text{F}_5)_4$  (**2**) (with added triphenylphosphine to stimulate solution conditions).

**O-Atom Transfer (OAT) Mechanism. Oxidation of Triphenylphosphine.** In the presence of substrates (e.g.,  $\text{PPh}_3$ ,  $\text{P}(\text{OR})_3$ , or  $\text{S}(\text{CH}_3)_2$ ), the photolysis of  $[(\text{P})\text{Fe}^{\text{III}}]_2\text{O}$  systems results in OAT, from a transient high-valent  $\text{Fe}^{\text{IV}}=\text{O}$ , to substrates.<sup>1,3,18</sup> By analogy,  $\text{PPh}_3$  oxygenation most likely occurs via a reactive mixed-valent species, either  $[(^6L)\text{Fe}^{\text{IV}}=\text{O}\cdots\text{Fe}^{\text{II}}\text{--Cl}]^+$  or  $[(^6L)\text{Fe}^{\text{II}}\cdots\text{O}=\text{Fe}^{\text{IV}}\text{--Cl}]^+$ . The so-formed high-valent  $\text{Fe}^{\text{IV}}=\text{O}$  intermediate is the result of the photodisproportionation of  $[(^6L)\text{Fe}^{\text{III}}\text{--O--Fe}^{\text{III}}\text{--Cl}]^+$  (**1**). Concomitant with OAT from  $[(^6L)\text{Fe}^{\text{IV}}=\text{O}\cdots\text{Fe}^{\text{II}}\text{--Cl}]^+$  or  $[(^6L)\text{Fe}^{\text{II}}\cdots\text{O}=\text{Fe}^{\text{IV}}\text{--Cl}]^+$  is the observed diferrous complex  $[(^6L)\text{Fe}^{\text{II}}\cdots\text{Fe}^{\text{II}}\text{--Cl}]\text{B}(\text{C}_6\text{F}_5)_4$  (**2**). Further discussion of whether a heme or non-heme  $\text{Fe}^{\text{IV}}=\text{O}$  moiety forms in the present system is given below. In the absence of a substrate, the transiently generated  $\text{Fe}(\text{IV})/\text{Fe}(\text{II})$  species would decay rapidly back to the ground state. Such conproportionation chemistry is similar to what has been reported for  $\mu$ -oxo bridged  $\text{Fe}^{\text{III}}\text{--O--Fe}^{\text{III}}$  cofacial porphyrin sandwich complexes that are irradiated in benzene solutions in the absence of triphenylphosphine, where the lack of suitable O-atom acceptor leads to no observed photoproduct,<sup>1</sup> since benzene solvent is not an oxidizable substrate in this system.

**Photolysis of  $[(^6L)\text{Fe}^{\text{III}}\text{--O--Fe}^{\text{III}}\text{--Cl}]^+$  (**1**) in THF.** When THF solutions of  $[(^6L)\text{Fe}^{\text{III}}\text{--O--Fe}^{\text{III}}\text{--Cl}]^+$  (**1**) were

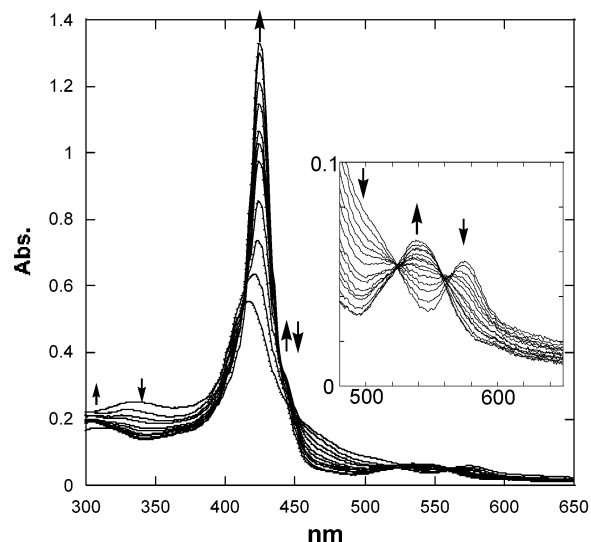


**Figure 2.** Photoreduction of  $[(^6L)\text{Fe}^{\text{III}}\text{--O--Fe}^{\text{III}}\text{--Cl}]^+$  (**1**)  $\{\lambda_{\text{max}} 328, 416$  (Soret), and  $570 \text{ nm}\}$  to form  $[(^6L)\text{Fe}^{\text{II}}\cdots\text{Fe}^{\text{II}}\text{--Cl}]\text{B}(\text{C}_6\text{F}_5)_4$  (**2**)  $\{\lambda_{\text{max}} 318, 424$  (Soret), and  $545 \text{ nm}\}$  under an  $\text{N}_2$  atmosphere in THF at  $293 \text{ K}$ . The spectra were recorded at  $\sim 5 \text{ min}$  intervals over the course of  $1 \text{ h}$ .

photolyzed under an  $\text{N}_2$  atmosphere, using similar conditions to those listed above for benzene but without the addition of triphenylphosphine, we observed the rapid ( $\sim 1 \text{ h}$ ) photoreduction of **1** to  $[(^6L)\text{Fe}^{\text{II}}\cdots\text{Fe}^{\text{II}}\text{--Cl}]\text{B}(\text{C}_6\text{F}_5)_4$  (**2**) (Scheme 1). Spectral changes, Figure 2, show a steady bleach of three electronic transitions centered at  $\lambda_{\text{max}} \sim 330, 416,$  and  $570 \text{ nm}$  which correspond to the charge-transfer, Soret, and Q-band transitions (respectively) in the UV–vis spectrum of  $[(^6L)\text{Fe}^{\text{III}}\text{--O--Fe}^{\text{III}}\text{--Cl}]^+$  (**1**). Concomitant growth of peaks at  $\lambda_{\text{max}} 424$  and  $545 \text{ nm}$ , due to formation of  $[(^6L)\text{Fe}^{\text{II}}\cdots\text{Fe}^{\text{II}}\text{--Cl}]\text{B}(\text{C}_6\text{F}_5)_4$  (**2**), occurs. During the course of photolysis, we also observed the transient formation of a shoulder at  $\lambda_{\text{max}} 440 \text{ nm}$ , which typically disappeared within  $\sim 5 \text{ min}$  of photolysis termination. Monitoring the dark reaction for the decay of the peak at  $440 \text{ nm}$  revealed a steady but equal (in intensity) increase in absorption for the Soret band of **2** ( $\lambda_{\text{max}} = 424 \text{ nm}$ ). It thus appears that photochemically derived species undergo a slow dark transformation to give the final diferrous product  $[(^6L)\text{Fe}^{\text{II}}\cdots\text{Fe}^{\text{II}}\text{--Cl}]\text{B}(\text{C}_6\text{F}_5)_4$  (**2**). With knowledge of molar extinction coefficients for both **1** and **2** in THF solvent,<sup>8,12</sup> it could be determined that the photochemically induced reduction of **1** to **2** occurs in excellent yield ( $\sim 99\%$ ).

The photoproduction of  $[(^6L)\text{Fe}^{\text{II}}\cdots\text{Fe}^{\text{II}}\text{--Cl}]\text{B}(\text{C}_6\text{F}_5)_4$  (**2**) from **1**, in the absence of an obvious O-atom acceptor such as triphenylphosphine, suggests that something else in solution is being oxidized. Indeed, an analysis of the organic reaction products led us to observe the formation of  $\gamma$ -butyrolactone in low yield ( $\sim 15\%$  based on the initial concentration of **1**). The formation of this carbonyl product, which represents a THF molecule that has been oxidized in an overall four-electron process, was rather puzzling. We did not see the formation of the corresponding 2-hydroxy-THF (an “intermediate” two-electron oxidized product, similar to what has been suggested for THF oxidation by

(18) Pistorio, B. J.; Chang, C. J.; Nocera, D. G. *J. Am. Chem. Soc.* **2002**, *124*, 7884–7885.

high-valent copper–oxygen species),<sup>19</sup> suggesting that over-oxidation of a preliminary alcohol product was unlikely. Likewise, the photolysis of THF solutions of  $[(^6\text{L})\text{Fe}^{\text{III}}-\text{O}-\text{Fe}^{\text{III}}-\text{Cl}]^+$  (**1**) charged with 1 atm of dioxygen resulted in the formation of  $\gamma$ -butyrolactone in similar quantities. However, the aerobic photolysis reactions did not result in the buildup of the photoreduced species  $[(^6\text{L})\text{Fe}^{\text{II}}\cdots\text{Fe}^{\text{II}}-\text{Cl}]\text{B}(\text{C}_6\text{F}_5)_4$  (**2**), as expected, since it would reoxidize to **1** (vide supra).

To determine whether the O-atom in the lactone product was directly derived from the O-atom of the  $\mu$ -oxo bridge of  $[(^6\text{L})\text{Fe}^{\text{III}}-\text{O}-\text{Fe}^{\text{III}}-\text{Cl}]^+$  (**1**),  $[(^6\text{L})\text{Fe}^{\text{III}}-(^{18}\text{O})-\text{Fe}^{\text{III}}-\text{Cl}]\text{B}(\text{C}_6\text{F}_5)_4$  (**1-<sup>18</sup>O**) was utilized in a THF solvent photolysis. However, GC–MS analysis showed that no <sup>18</sup>O-atom incorporation into the  $\gamma$ -butyrolactone product was observed. An investigation of the products derived from exposure to <sup>18</sup>O<sub>2</sub>(g) was then undertaken to better understand the role of dioxygen in the observed oxidation chemistry. A reaction mixture photolyzed under anaerobic conditions was directly bubbled with <sup>18</sup>O<sub>2</sub> prior to opening to the atmosphere and subsequent workup. It was discovered that the  $\gamma$ -butyrolactone product showed <sup>18</sup>O-incorporation ( $m/z$  88; ~90% incorporation). Likewise, the 1 h photolysis of THF solutions of  $[(^6\text{L})\text{Fe}^{\text{III}}-\text{O}-\text{Fe}^{\text{III}}-\text{Cl}]^+$  (**1**), charged with 1 atm of <sup>18</sup>O<sub>2</sub>, resulted in the similar formation of <sup>18</sup>O-labeled  $\gamma$ -butyrolactone. These observations suggest that radical species derived from THF, either bound to iron or free in solution, are combining with dioxygen to give the observed  $\gamma$ -butyrolactone as an auto-oxidation product. The remaining THF radicals likely polymerize in solution, resulting in the formation of intractable material.

**Photolysis of  $[(^6\text{L})\text{Fe}^{\text{III}}-\text{O}-\text{Fe}^{\text{III}}-\text{Cl}]^+$  (**1**) in Toluene.** The anaerobic photolysis of toluene solutions of  $[(^6\text{L})\text{Fe}^{\text{III}}-\text{O}-\text{Fe}^{\text{III}}-\text{Cl}]^+$  (**1**) also yields  $[(^6\text{L})\text{Fe}^{\text{II}}\cdots\text{Fe}^{\text{II}}-\text{Cl}]\text{B}(\text{C}_6\text{F}_5)_4$  (**2**), as determined by UV–vis spectroscopic monitoring of the reaction (Supporting Information, Figure S2). The absorbance spectrum for **2**, obtained during the course of these photoreductions, is identical to the electronic spectrum of an authentic sample of  $[(^6\text{L})\text{Fe}^{\text{II}}\cdots\text{Fe}^{\text{II}}-\text{Cl}]\text{B}(\text{C}_6\text{F}_5)_4$  (**2**) that is prepared in deoxygenated toluene. The most dramatic absorbance changes occur with the loss of the signal corresponding to the high energy LMCT ( $\lambda_{\text{max}}$  330 nm) and a splitting in the Soret and Q-band regions into two peaks. The re-exposure of these solutions to dioxygen resulted in the reformation of the  $\mu$ -oxo complex **1**. Using known molar extinction coefficients,<sup>8,12</sup> it could be determined that photochemically induced reduction of **1** to **2** occurs near quantitatively (~99%) in a mixed 10% THF/toluene solvent system (yielding both  $\gamma$ -butyrolactone and benzaldehyde). The mixed solvent system was needed due to the limited solubility of **1** and **2** in toluene. Unlike the case of photolysis of **1** in THF (vide supra), no dark reaction was observed.

Thus, similar to the observed photochemistry in THF solvent, the use of toluene solvent without an added O-atom acceptor resulted in noticeable anaerobic photochemistry. An

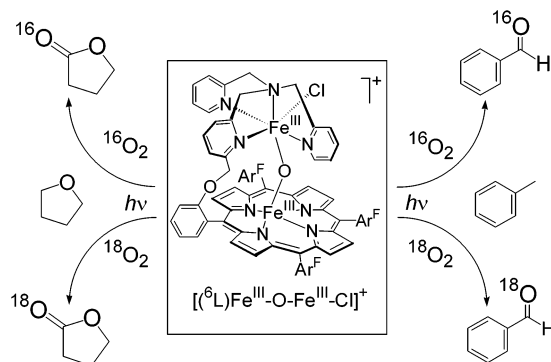


**Figure 3.** Dioxygen-derived organic oxidation products from both THF yielding  $\gamma$ -butyrolactone and toluene to give benzaldehyde. Note that bibenzyl is also observed as a product from the photolysis of **1** in toluene. See text for details.

analysis of the organic reaction products, after aerobic workup, revealed the formation of benzaldehyde (~23% yield based upon **1**) and the presence (<1%) of bibenzyl. Similar to the case of THF, we did not observe the formation of benzyl alcohol under these conditions, suggesting that overoxidation of an initially formed alcohol product was unlikely. Anaerobic toluene solutions of  $[(^6\text{L})\text{Fe}^{\text{III}}-(^{18}\text{O})-\text{Fe}^{\text{III}}-\text{Cl}]\text{B}(\text{C}_6\text{F}_5)_4$  (**1-<sup>18</sup>O**) did not lead to <sup>18</sup>O-atom incorporation into the benzaldehyde photolysis products. As in the case of THF oxidation to a lactone, the four-electron oxidation of toluene to benzaldehyde involves a mechanism that is more complicated than a direct O-atom transfer (OAT) reaction from a high valent Fe–oxo complex to a substrate, to be discussed further below. A summary of the dioxygen derived photoproducts is shown in Figure 3.

The product quantum yields for the photoreduction of  $[(^6\text{L})\text{Fe}^{\text{III}}-\text{O}-\text{Fe}^{\text{III}}-\text{Cl}]^+$  (**1**) in both THF and toluene solutions were determined by actinometry. The efficiency of this reaction, measured by the appearance of the fully reduced complex  $[(^6\text{L})\text{Fe}^{\text{II}}\cdots\text{Fe}^{\text{II}}-\text{Cl}]\text{B}(\text{C}_6\text{F}_5)_4$  (**2**), is affected by the solvent. In the coordinating solvent THF, the  $\Phi_{\text{p}}$  value was  $7.1 \times 10^{-5}$  while in the noncoordinating solvent toluene we obtained a  $\Phi_{\text{p}}$  value of  $3.25 \times 10^{-6}$ . Product quantum yields in the range of  $\Phi_{\text{p}} = 10^{-4}$ – $10^{-8}$  are typically found for the photoreduction of  $\mu$ -oxo bridged  $[(\text{P})\text{Fe}]_2\text{O}$  compounds.<sup>1–3,18</sup>

**Aerobic Oxidation in THF and Toluene. Photobleach Products.** When dioxygen-saturated THF or toluene solutions of  $[(^6\text{L})\text{Fe}^{\text{III}}-\text{O}-\text{Fe}^{\text{III}}-\text{Cl}]^+$  (**1**) were subjected to photolysis, using similar reaction conditions to the anaerobic photolysis reactions described above, we did not observe the buildup of a new metal complex photoproduct. However, the photolysis of these solutions (THF or toluene) for 24 h resulted in the complete bleaching of the solutions as evidenced by loss of all UV–vis absorbance features. Scrutiny of the organic products obtained from these reactions gives similar results, but in higher yields, to the corresponding anaerobic photolysis reactions. In the case of THF, we observed several turnovers ( $5 \pm 1$ ) of the cyclic ether to  $\gamma$ -butyrolactone ( $m/z$  86 amu). When THF solutions were saturated using labeled <sup>18</sup>O<sub>2</sub>, we observed incorporation of an <sup>18</sup>O-atom into the  $\gamma$ -butyrolactone ( $m/z$  88 amu; 90%)

(19) Zhang, C. X.; Liang, H.-C.; Kim, E.-i.; Shearer, J.; Helton, M. E.; Kim, E.; Kaderli, S.; Incarvito, C. D.; Zuberbuehler, A. D.; Rheingold, A. L.; Karlin, K. D. *J. Am. Chem. Soc.* **2003**, *125*, 634–635.

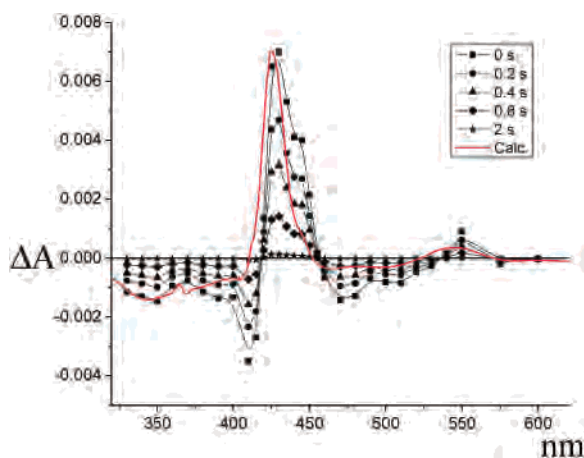


**Figure 4.** Transient absorption spectra recorded during the laser flash photolysis ( $\lambda_{\text{ex}} = 355 \text{ nm}$ ; 198 K) of  $[(^6\text{L})\text{Fe}^{\text{III}}\text{-O-Fe}^{\text{III}}\text{-Cl}]^+$  (**1**) in THF.

suggesting that the source of oxygen in the products is dioxygen, introduced into the system following aerobic workup (see Experimental Section) and not from OAT from a photogenerated reactive intermediate derived from the  $\mu$ -oxo bridged complex  $[(^6\text{L})\text{Fe}^{\text{III}}\text{-O-Fe}^{\text{III}}\text{-Cl}]^+$  (**1**).

In the case of toluene, the organic products include benzaldehyde ( $m/z$  106 amu) and bibenzyl ( $m/z$  182 amu), however, in very few turnovers ( $2 \pm 1$ ) under these aerobic conditions. A careful examination of the crude reaction mixture, using thin-layer chromatography, also revealed the presence of benzoic acid (which adheres to the baseline) suggesting that an overoxidation of benzaldehyde occurs during the course of prolonged aerobic photolysis reactions in toluene. Thus, it is difficult to ascertain the exact turnover number for the photoproduction of benzaldehyde from toluene, given the reaction and workup conditions employed for analysis. The C–C coupled product bibenzyl, which is commonly found as the concentration of benzyl radical in solution increases, is also observed in good yield ( $16 \pm 2$  turnovers) under these conditions. The clear presence of benzyl radicals in solution suggests that an initially formed high-valent Fe–oxo species homolytically cleaves the benzylic C–H bond of toluene.

**Transient Absorption Spectroscopy.** To probe the nature of any transiently formed high-valent Fe(IV) species and in an attempt to possibly differentiate between a heme versus non-heme  $\text{Fe}^{\text{IV}}\text{=O}$  intermediate in our system, we undertook transient absorption (TA) spectroscopic measurements. TA spectra of  $[(^6\text{L})\text{Fe}^{\text{III}}\text{-O-Fe}^{\text{III}}\text{-Cl}]^+$  (**1**) are shown in Figure 4, recorded in an anaerobic THF solution at 198 K. Transient bleaches of the charge-transfer region ( $\lambda_{\text{max}} \sim 340 \text{ nm}$ ), the Soret region ( $\lambda_{\text{max}} \sim 415 \text{ nm}$ ), and the Q-band domain ( $\lambda_{\text{max}} \sim 470, 500, 575 \text{ nm}$ ) are coupled to transient absorbances in the Soret ( $\lambda_{\text{max}} \sim 430 \text{ nm}$ ) and Q-band ( $\lambda_{\text{max}} \sim 550 \text{ nm}$ ) areas. They reveal the presence of a short-lived porphyrin species with features ( $\lambda_{\text{max}} 427, 445 \text{ (sh)}, 552 \text{ nm}$ ) that are very strongly suggestive of a transient Fe(II)-like porphyrin complex<sup>20,21</sup> that decays back to the starting

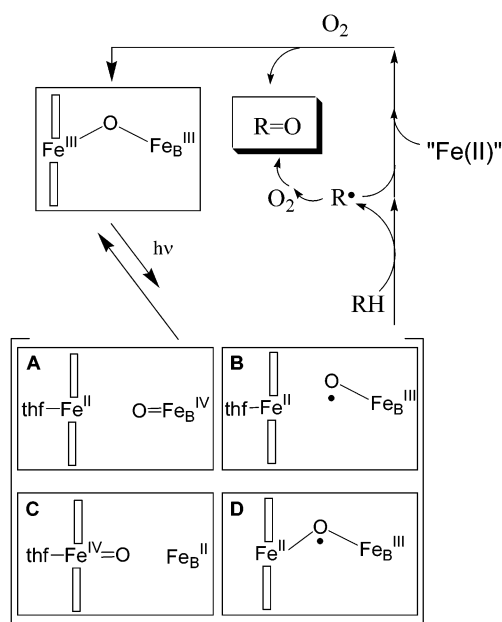


**Figure 5.** Proposed photocatalytic cycle for  $[(^6\text{L})\text{Fe}^{\text{III}}\text{-O-Fe}^{\text{III}}\text{-Cl}]^+$  (**1**) in THF or toluene (RH) solvents. The cycle begins with the reversible photolysis of  $[(^6\text{L})\text{Fe}^{\text{III}}\text{-O-Fe}^{\text{III}}\text{-Cl}]^+$  (**1**) (upper left) producing an Fe–oxo intermediate capable of H-atom abstraction. The subsequently formed alkyl radicals ultimately react with dioxygen to yield the observed carbonyl products (see text for further details).

$\mu$ -oxo complex after 2 s. The calculated difference spectrum  $[A_{[(^6\text{L})\text{Fe}^{\text{II}}\text{...Fe}^{\text{III}}\text{-Cl}]\text{B}(\text{C}_6\text{F}_5)_4(2)} - A_{[(^6\text{L})\text{Fe}^{\text{III}}\text{-O-Fe}^{\text{III}}\text{-Cl}]^+(1)}]$  is shown as the dark solid trace in Figure 4. This matches closely the experimentally obtained TA spectra which is similar to (P)Fe<sup>II</sup> species in coordinating solvents.<sup>20,21</sup> In THF solvent, the cyclic ether acts as an axial ligand base and may further stabilize the formation of heme–Fe<sup>II</sup> transient species.<sup>20,21</sup>

The nature of this transient species (Figure 5) is likely a photoproduct of  $\text{O} \rightarrow \text{Fe}$  LMCT excitation. Four photoproducts which may be discussed are labeled **A–D**, Figure 5. In the case of a formal photodissociated Fe<sup>II</sup>/Fe<sup>IV</sup>=O pair (**A** or **C**), species **A** involving a transiently formed ferrous heme is more likely based on TA data. However, we can also consider the possibility that the photoproduct is a mixed valent Fe<sup>II</sup>/Fe<sup>III</sup> pair which is better formulated as either **D** (a short-lived oxyl radical photoproduct following LMCT excitation) or **B** (essentially a resonance structure alternate description of **A**, with the non-heme Fe–oxo treated as a radical leaving group). Note that the reaction was performed at 198 K to prevent extensive reaction of the transiently formed species with the THF solvent.

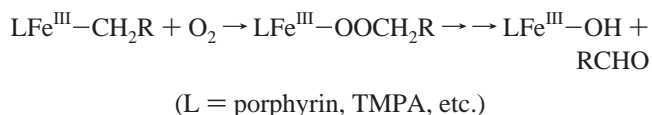
**Mechanistic Considerations. Solvent Oxidation.** A possible photocatalytic mechanism, accounting for the formation (in multiple turnovers) of the four-electron oxidized products such as those observed here in THF and toluene, is presented in Figure 5. Photoexcitation of  $[(^6\text{L})\text{Fe}^{\text{III}}\text{-O-Fe}^{\text{III}}\text{-Cl}]^+$  (**1**) yields one or more charge-separated configurations depicted as **A–D**. States **A** and **C** are analogous to the possibilities suggested above for the photochemistry in the presence of triphenylphosphine (vide supra). With evidence from TA data

(20) Ghiladi, R. A.; Kretzer, R. M.; Guzei, I.; Rheingold, A. L.; Neuhold, Y.-M.; Hatwell, K. R.; Zuberbuehler, A. D.; Karlin, K. D. *Inorg. Chem.* **2001**, *40*, 5754–5767.

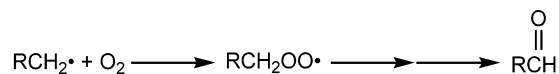
(21) Ghiladi, R. A.; Karlin, K. D. *Inorg. Chem.* **2002**, *41*, 2400–2407.

discussed (vide supra), we suspect that configuration C can likely be ruled out as a transient intermediate. Whichever is an active intermediate, they would all be good candidates for H-atom abstraction from C–H bonds in hydrocarbons such as THF or toluene. Oxo–iron (IV) porphyrin complexes normally are considered not to be good H-atom abstraction agents, but with electron-deficient ligands Nam and co-workers have recently shown that they are capable of C–H bond activation in a manner similar to the reactivity of the oxo–iron (IV) porphyrin radical cations.<sup>22,23</sup> Similarly, synthetic non-heme oxo–iron (IV) species have been shown to be powerful oxidants capable of C–H bond cleavage.<sup>9–11,24</sup> As such, we suggest that the photochemically generated non-heme Fe–oxo species abstracts an H-atom from THF or toluene, initiating a radical chain reaction by forming a THF or benzyl radical. The radical species are free to slowly (under these dilute conditions) dimerize, as observed in the case of toluene oxidation which would generate benzyl radical (leading to bibenzyl product). We must also consider the possibility that low-valent Fe(II) sites (Figure 5) might act as radical “traps” by, in this case, forming Fe(III)–alkyl (e.g., Fe<sup>III</sup>–η<sup>1</sup>-(C<sub>4</sub>H<sub>7</sub>O) from THF) or Fe(III)–benzyl complexes.<sup>23,25–27</sup> Such species are unstable in the presence of dioxygen workup and/or aerobic photoreactions, forming the corresponding Fe(III)–OH coordination species along with carbonyl compounds (see equation that follows).<sup>25–28</sup> Alternatively, free radicals in solution might directly combine with dioxygen and ultimately lead to the observed carbonyl products via an auto-oxidation pathway (see below). Thus, it is likely that the formation of the four-electron oxidized products  $\gamma$ -butyrolactone (from THF oxidation) and benzaldehyde (from toluene oxidation) are a result of aerobic workup, where either free-radical species or ferric–alkyl species react with dioxygen to give the corresponding carbonyl compounds.<sup>4,25,28</sup> Since alcohol products were not detected during the course of reaction, we can rule out the possibility of a rebound-type mechanism, similar to what is typically seen in cytochrome P-450 systems.<sup>4,5</sup> It should be noted that in the event of intermediate formation of a (P)–Fe<sup>III</sup>–OH or (P)Fe<sup>III</sup>–R complex, the resulting photolability of these species could also lead to the corresponding hydroxyl radical or alkyl radical.<sup>23,25–28</sup> It is likely that the presence of hydroxyl radical leads to the degradation of the complex [(<sup>6</sup>L)Fe<sup>III</sup>–O–Fe<sup>III</sup>–Cl]<sup>+</sup> (**1**) during the course of prolonged aerobic photolysis. Finally, <sup>18</sup>O-label incorporation was achieved only upon workup (or reaction) in the presence of <sup>18</sup>O<sub>2</sub>(g). Thus, while the  $\mu$ -oxo complex **1** likely initiates

radical chemistry, dioxygen serves as the O-atom source in the products observed.



or



**Dechlorination Reactions via Photolysis of [(<sup>6</sup>L)Fe<sup>III</sup>–O–Fe<sup>III</sup>–Cl]<sup>+</sup> (**1**).** From the standpoint of environmental chemistry, the dehalogenation of chlorinated compounds is of profound importance. Specifically, chlorinated benzene compounds have found widespread use as solvents and pesticides and as a result have become contaminants of terrestrial water and soil,<sup>29</sup> while R–X compounds in general are designated as priority pollutants by USEPA.<sup>30</sup> As there is precedent for biological heme or non-heme diiron–oxo mediated oxidative chlorocarbon degradation with enzymes such as cytochrome P-450 and methane monooxygenase,<sup>6,23,31,32</sup> we sought to explore the use of [(<sup>6</sup>L)Fe<sup>III</sup>–O–Fe<sup>III</sup>–Cl]<sup>+</sup> (**1**) for such chemistry.

**Benzyl Chloride Dehalogenation.** This chlorocarbon compound was tested as a substrate in anticipation of its likely being an “easy” substrate, but one for which reaction products could be easily identified. Neither anaerobic nor aerobic photolysis of benzene solutions of [(<sup>6</sup>L)Fe<sup>III</sup>–O–Fe<sup>III</sup>–Cl]<sup>+</sup> (**1**) in the presence of 1 M benzyl chloride resulted in the buildup of any photoreduced species. However, spectroscopic monitoring of reaction solutions showed that the UV–vis bands from [(<sup>6</sup>L)Fe<sup>III</sup>–O–Fe<sup>III</sup>–Cl]<sup>+</sup> (**1**) { $\lambda_{\text{max}}$  334, 418 (Soret), 574 nm} were replaced by absorptions characteristic of a chloride porphyrinate iron(III) (i.e., (P)–Fe<sup>III</sup>–Cl) moiety { $\lambda_{\text{max}}$  378, 418 (Soret), 507, 648 nm} (Figure 6).<sup>20,33</sup> The identification and characterization of the iron chloride-containing product found is given below. Benzaldehyde (~70%) was found to be the oxidative dechlorination product, and no evidence was found to suggest the presence of bibenzyl. Scenarios for the possible mechanism of formation of benzaldehyde are mentioned below.

**Chlorobenzene and Dichlorobenzene Dehalogenation.** Chloroaromatics are persistent environmental pollutants.<sup>30</sup> As 1,2-dichlorobenzene and chlorobenzene could also serve as solvents for reaction, we examined the photolytic reactions with [(<sup>6</sup>L)Fe<sup>III</sup>–O–Fe<sup>III</sup>–Cl]<sup>+</sup> (**1**). For the photolysis of **1** in neat 1,2-dichlorobenzene, UV–vis spectroscopic changes made it evident that a (P)Fe<sup>III</sup>–Cl containing species was formed. Similarly, the photolysis of chlorobenzene solutions

(22) Nam, W.; Park, S.-E.; Lim, I. K.; Lim, M. H.; Hong, J.; Kim, J. *J. Am. Chem. Soc.* **2003**, *125*, 14674–14675.

(23) Maldotti, A.; Amadelli, R.; Bartocci, C.; Carassiti, V.; Polo, E.; Varani, G. *Coord. Chem. Rev.* **1993**, *125*, 143–154.

(24) Costas, M.; Rohde, J.-U.; Stubna, A.; Ho, R. Y. N.; Quaroni, L.; Muenck, E.; Que, L., Jr. *J. Am. Chem. Soc.* **2001**, *123*, 12931–12932.

(25) Arasasingham, R. D.; Balch, A. L.; Cormman, C. R.; Latos-Grazynski, L. *J. Am. Chem. Soc.* **1989**, *111*, 4357–4363.

(26) Johnston, M. D. In *Comprehensive Organometallic Chemistry*; Wilkinson, G., Stone, F. G. A., Abel, E. W., Eds.; Pergamon Press: New York, 1982; Vol. 4.

(27) Shin, K.; Yu, B.-S.; Goff, H. M. *Inorg. Chem.* **1990**, *29*, 889–890.

(28) Balch, A. L.; Hart, R. L.; Latos-Grazynski, L.; Traylor, T. G. *J. Am. Chem. Soc.* **1990**, *112*, 7382–7388.

(29) Nowak, J.; Kirsch, N. H.; Hegemann, W.; Stan, H.-J. *Appl. Microbiol. Biotechnol.* **1996**, *45*, 700–709.

(30) USEPA. *40 CFR Part 131*; 1997; pp 42159–42208.

(31) Fox, B. G.; Borneman, J. G.; Wackett, L. P.; Lipscomb, J. D. *Biochemistry* **1990**, *29*, 6419–6427.

(32) T sien, H.-C.; Brusseau, G. A.; Hanson, R. S.; Wackett, L. P. *Appl. Environ. Microbiol.* **1989**, *55*, 3155–3161.

(33) Groves, J. T.; Nemo, T. E. *J. Am. Chem. Soc.* **1983**, *105*, 6243–6248.

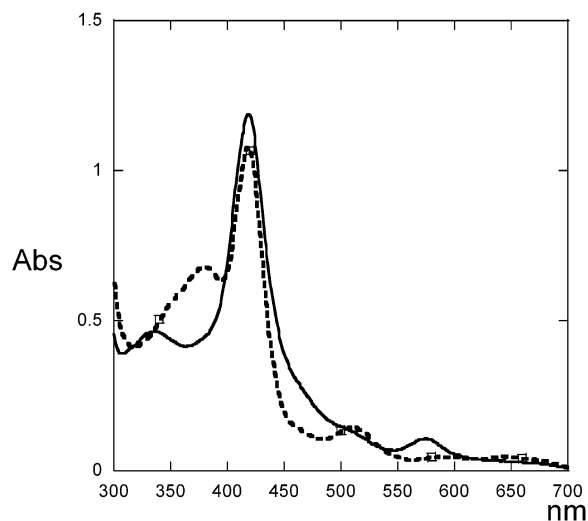
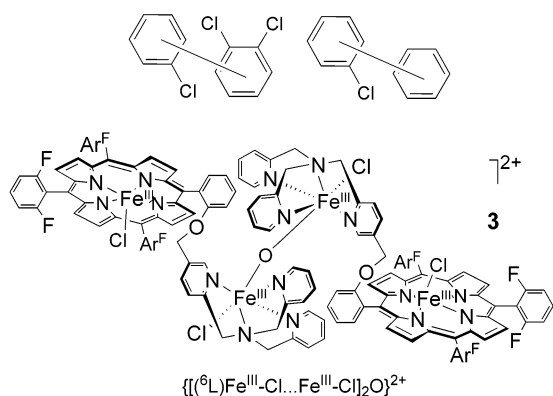


**Figure 6.** UV-vis spectra of  $[(^6\text{L})\text{Fe}^{\text{III}}-\text{O}-\text{Fe}^{\text{III}}-\text{Cl}]^+$  (**1**) (—) and the resulting photolysis product (---), (P) $\text{Fe}^{\text{III}}-\text{Cl}$  containing species **3** (see text).

**Chart 2**



of  $[(^6\text{L})\text{Fe}^{\text{III}}-\text{O}-\text{Fe}^{\text{III}}-\text{Cl}]^+$  (**1**) resulted in the formation of an identical (P) $\text{Fe}^{\text{III}}-\text{Cl}$  containing complex. The UV-vis spectra from the products of these two reactions matched the spectra from the reaction in benzene/benzyl chloride, as described above.

An analysis of the organic, and presumably dehalogenated, reaction products was undertaken. For reactions in 1,2-dichlorobenzene, the identifiable organic products included two isomers (corresponding to two new GC-MS peaks with the same  $m/z$ ) with the chemical formula  $\text{C}_{12}\text{H}_7\text{Cl}_3$  ( $m/z$  258 with isotope pattern consistent with this formulation; Supporting Information, Figure S3); the probable structures are shown in Chart 2. Similarly, photolysis reactions conducted in chlorobenzene resulted in the formation of two organic dehalogenation products with the chemical formula  $\text{C}_{12}\text{H}_9\text{Cl}$  ( $m/z$  189 with isotope pattern consistent with this formulation; Supporting Information, Figure S4); the structures of which are shown in Chart 2. As authentic samples of these biphenyl products were not available, information in regards to the phenyl substitution pattern or exact yield of organic product formation was not possible. In any case, the formation of these products represents a dehalogenation and coupling of chlorinated aromatic compounds. Both C-Cl and C-H bond activation and cleavage occur, presumably

involving the photochemically generated Fe-oxo species derived from  $[(^6\text{L})\text{Fe}^{\text{III}}-\text{O}-\text{Fe}^{\text{III}}-\text{Cl}]^+$  (**1**).

**Characterization of the  $\{[(^6\text{L})\text{Fe}^{\text{III}}-\text{Cl}\cdots\text{Fe}^{\text{III}}-\text{Cl}]_2\text{O}\}^{2+}$  Product (**3**). Fate of the Chlorine Atom.** The common product from the photolysis reactions of  $[(^6\text{L})\text{Fe}^{\text{III}}-\text{O}-\text{Fe}^{\text{III}}-\text{Cl}]^+$  (**1**) performed in chlorinated solvents (or with benzyl chloride/benzene) is the complex  $\{[(^6\text{L})\text{Fe}^{\text{III}}-\text{Cl}\cdots\text{Fe}^{\text{III}}-\text{Cl}]_2\text{O}\}^{2+}$  (**3**). The UV-vis spectrum of synthetically isolated  $\{[(^6\text{L})\text{Fe}^{\text{III}}-\text{Cl}\cdots\text{Fe}^{\text{III}}-\text{Cl}]_2\text{O}\}^{2+}$  (**3**) in  $\text{CH}_2\text{Cl}_2$   $\{\lambda_{\text{max}}$  375, 416 (Soret), 508, 576, 650 nm $\}$  from a 1,2-dichlorobenzene reaction (see Experimental Section) is identical to the spectrum of the solutions obtained after photolysis of  $[(^6\text{L})\text{Fe}^{\text{III}}-\text{O}-\text{Fe}^{\text{III}}-\text{Cl}]^+$  (**1**) in chlorobenzene, dichlorobenzene, or benzene/benzyl chloride. The absorbance in the charge-transfer region ( $\lambda_{\text{max}} \sim 380$  nm) is typical of both (P) $\text{Fe}^{\text{III}}-\text{Cl}$  complexes and non-heme diiron(III)  $[(\text{TPMA})\text{Fe}^{\text{III}}-\text{Cl}]_2\text{O}^{2+}$  complexes  $\{\text{TPMA} = \text{tris-pyridin-2-ylmethylamine}\}$ .<sup>33-35</sup> A porphyrin-base Soret transition at  $\lambda_{\text{max}} = 416$  nm coupled with Q-bands centered at  $\lambda_{\text{max}} = 508, 576,$  and 650 nm is also consistent with a high spin (P) $\text{Fe}^{\text{III}}-\text{Cl}$  formulation.<sup>33</sup> Elemental analysis suggests that the formulation  $\{[(^6\text{L})\text{Fe}^{\text{III}}-\text{Cl}\cdots\text{Fe}^{\text{III}}-\text{Cl}]_2\text{O}\}^{2+}$  (**3**) is correct, with solvation of 2 equiv of water. This formulation is further supported by ESI-MS measurements, which showed an  $m/z$  1221 species corresponding to the cation  $[(^6\text{L})\text{Fe}-\text{Cl}\cdots\text{Fe}-\text{Cl}]^+$  derived from the cleavage of the non-heme Fe-O-Fe bond (Supporting Information, Figure S5). An additional peak, as a result of methanol coordination to the non-heme Fe site, accounts for the peak found at  $m/z$  1251  $[(^6\text{L})\text{Fe}-\text{Cl}\cdots\text{Fe}(\text{OMe})-\text{Cl}]^+$ . The adventitious reaction of  $\{[(^6\text{L})\text{Fe}^{\text{III}}-\text{Cl}\cdots\text{Fe}^{\text{III}}-\text{Cl}]_2\text{O}\}^{2+}$  (**3**) with methanol, a solvent used for ESI mass spectrometry, is not surprising given the fact that  $[(^6\text{L})\text{Fe}^{\text{III}}-\text{O}-\text{Fe}^{\text{III}}-\text{Cl}]^+$  (**1**) has been shown to react with methanol and form an iron-methoxy complex.<sup>8</sup>  $^1\text{H}$  NMR spectroscopic investigation of **3** reveals a signal at  $\delta$  81 ppm and is assigned as a pyrrole proton peak highly characteristic of a high-spin (P) $\text{Fe}^{\text{III}}-\text{Cl}$  complex (Supporting Information, Figure S6).<sup>36,37</sup> Additional multiplet signals found at  $\delta$  14.14, 12.8, 6.92, and 6.83 ppm are derived from pyridyl proton resonances that stem from the TPMA-Fe moiety (Supporting Information, Figure S7).<sup>35</sup> Such signals, in the diamagnetic region, are consistent with either low spin ferrous TPMA-like systems or antiferromagnetically coupled  $\text{Fe}^{\text{III}}-\text{O}-\text{Fe}^{\text{III}}$  complexes, as described by Que, Jr., and co-workers.<sup>34,38</sup> Given the combined  $^1\text{H}$  NMR, elemental, and mass spectral data, it is likely that the non-heme iron site is an antiferromagnetically coupled non-heme  $\text{Fe}^{\text{III}}-\text{O}-\text{Fe}^{\text{III}}$  species. Unfortunately, we have been unsuccessful at growing X-ray quality crystals of  $\{[(^6\text{L})\text{Fe}^{\text{III}}-\text{Cl}\cdots\text{Fe}^{\text{III}}-\text{Cl}]_2\text{O}\}^{2+}$  (**3**), which would have helped to absolutely confirm this structural

(34) Zang, Y.; Kim, J.; Dong, Y.; Wilkinson, E. C.; Appelman, E. H.; Que, L., Jr. *J. Am. Chem. Soc.* **1997**, *119*, 4197-4205.

(35) Kojima, T.; Leising, R. A.; Yan, S.; Que, L., Jr. *J. Am. Chem. Soc.* **1993**, *115*, 11328-11335.

(36) Karlin, K. D.; Nanthakumar, A.; Fox, S.; Murthy, N. N.; Ravi, N.; Huynh, B. H.; Orosz, R. D.; Day, E. P. *J. Am. Chem. Soc.* **1994**, *116*, 4753-4763.

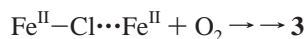
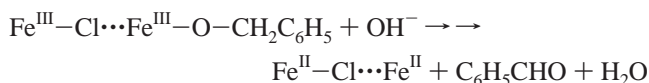
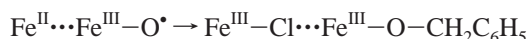
(37) Walker, F. A. In *Porphyrin Handbook*; Kadish, K. M., Smith, K. M., Guillard, R., Eds.; Academic Press: New York, 2000; Vol. 5.

(38) Chiou, Y.-M.; Que, L., Jr. *J. Am. Chem. Soc.* **1995**, *117*, 3999-4013.



assignment. Given that no other Fe products were obtained during the course of these reactions, it appears that the “new” chloride ligands in the complex  $\{[(^6\text{L})\text{Fe}^{\text{III}}-\text{Cl}\cdots\text{Fe}^{\text{III}}-\text{Cl}]_2\text{O}\}^{2+}$  (**3**) (relative to **1**) are derived from the solvent via the dechlorination reactions.

**Mechanistic Considerations. Photochemistry of  $[(^6\text{L})\text{Fe}^{\text{III}}-\text{O}-\text{Fe}^{\text{III}}-\text{Cl}]^+$  (**1**) in Benzene/Benzyl Chloride.** Unlike the cleavage of aromatic C–Cl bonds (BDE  $\sim$  97 kcal/mol) in the photolysis in neat chlorobenzene or 1,2-dichlorobenzene, benzylic C–Cl bonds are considerably weaker (BDE  $\sim$  74 kcal/mol). The lack of observable bibenzyl product (vide supra) suggests the absence of free benzyl radical during the course of reaction. Therefore, we propose that the initially formed high-valent iron–oxo photoproduct (see Figure 5) reacts in a concerted fashion with benzyl chloride producing a (P) $\text{Fe}^{\text{III}}-\text{Cl}\cdots\text{Fe}^{\text{III}}-\text{OCH}_2\text{C}_6\text{H}_5$  alkoxy species (see equation that follows). This reaction can also be thought of as occurring by combination of the  $\text{Fe}^{\text{II}}\cdots\text{Fe}^{\text{III}}-\text{O}^\bullet$  (Figure 5C) with the homolytic cleavage products of benzyl chloride (i.e.,  $\text{Cl}^\bullet$  and  $\text{C}_6\text{H}_5\text{CH}_2^\bullet$ ).  $\text{Fe}^{\text{III}}-\text{OCH}_2\text{C}_6\text{H}_5$  reacts with hydroxide (during alumina workup) producing a (formal) carbanion intermediate which rearranges to give benzaldehyde and reduced iron ( $\text{Fe}^{\text{II}}-\text{Cl}\cdots\text{Fe}^{\text{II}}$ ); the latter reoxidizes to  $\{[(^6\text{L})\text{Fe}^{\text{III}}-\text{Cl}\cdots\text{Fe}^{\text{III}}-\text{Cl}]_2\text{O}\}^{2+}$  (**3**) in the aerobic workup. We should note that so-formed  $^{18}\text{O}$ -labeled benzaldehyde, which should be produced from the photolysis of  $[(^6\text{L})\text{Fe}^{\text{III}}-(^{18}\text{O})-\text{Fe}^{\text{III}}-\text{Cl}]\text{B}(\text{C}_6\text{F}_5)_4$  (**1**- $^{18}\text{O}$ ) or by the photolysis of  $^{18}\text{O}_2$  saturated solutions of **1**, would rapidly exchange with water on the alumina, producing  $^{16}\text{O}$ -labeled benzaldehyde, as experimentally observed. The use of added  $\text{H}_2^{18}\text{O}$  in attempts to incorporate an  $^{18}\text{O}$ -labeled carbonyl into benzaldehyde was also unsuccessful, but we found that water strongly inhibited photochemistry in the first place.



**Mechanistic Considerations. Chloroaromatic Dehalogenation and Formation of **3**.** A proposed reaction pathway to account for the formation of  $\{[(^6\text{L})\text{Fe}^{\text{III}}-\text{Cl}\cdots\text{Fe}^{\text{III}}-\text{Cl}]_2\text{O}\}^{2+}$  (**3**), along with the dehalogenated and coupled organic products, is shown in Figure 7. Solutions of the  $\mu$ -oxo complex  $[(^6\text{L})\text{Fe}^{\text{III}}-\text{O}-\text{Fe}^{\text{III}}-\text{Cl}]^+$  (**1**), prepared in chlorobenzene or dichlorobenzene, are subjected to photolysis resulting in the formation of a reactive Fe–oxo intermediate. This species is likely capable of both aromatic C–H and C–Cl bond cleavage. In the case of chloride or chlorine atom abstraction, an  $\text{Fe}^{\text{III}}-\text{OCl}$  hypochlorite intermediate may form.<sup>39</sup> The observed biphenyl trichloride products represent a combination of processes, where the initially formed Fe–oxo species either cleaves a C–Cl bond or a C–H bond. The reaction products formed either under anaerobic or

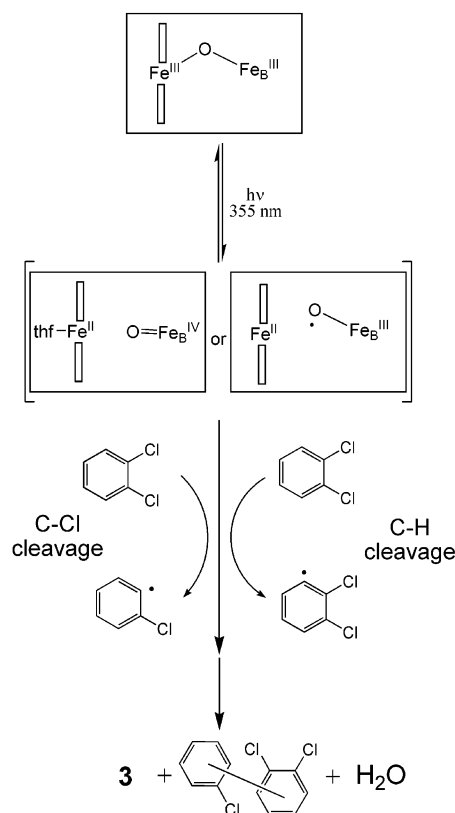


**Figure 7.** Proposed photochemically derived reaction pathway to account for the formation of a (P) $\text{Fe}^{\text{III}}-\text{Cl}$  product and the observed coupled, dehalogenated product. See text for further discussion.

aerobic photolysis reactions were the same, representing two substrate molecules which have been coupled with formal loss of HCl. It should be noted that the diferrous compound  $[(^6\text{L})\text{Fe}^{\text{II}}\cdots\text{Fe}^{\text{II}}-\text{Cl}]^+$  (**2**) is thermally stable in chlorobenzene and dichlorobenzene, so it is likely that **2** does not react with the halogenated solvent. The photochemical dehalogenation of substrates such as  $\text{CCl}_4$  by ethanol, photocatalyzed by hemes, has been proposed to involve formal HCl and  $\text{Cl}^\bullet$  species,<sup>40</sup> which are likely intermediates from our photochemistry, as well. In the event that a transiently photoreduced (P) $\text{Fe}^{\text{II}}$  species could react with dioxygen during the course of aerobic reactions, the product would be reformation of the parent  $[(^6\text{L})\text{Fe}^{\text{III}}-\text{O}-\text{Fe}^{\text{III}}-\text{Cl}]^+$  (**1**) and re-entry into the photocycle. The photoproduct  $\{[(^6\text{L})\text{Fe}^{\text{III}}-\text{Cl}\cdots\text{Fe}^{\text{III}}-\text{Cl}]_2\text{O}\}^{2+}$  (**3**) is neither photochemically active or reactive with dioxygen. It does, however, degrade (i.e., bleach) if prolonged photolysis is carried out.

## Summary and Conclusions

The heme/non-heme diiron  $\mu$ -oxo complex  $[(^6\text{L})\text{Fe}^{\text{III}}-\text{O}-\text{Fe}^{\text{III}}-\text{Cl}]^+$  (**1**) photoreduces, under anaerobic conditions, to give the corresponding diferrous compound  $[(^6\text{L})\text{Fe}^{\text{II}}\cdots\text{Fe}^{\text{II}}-\text{Cl}]\text{B}(\text{C}_6\text{F}_5)_4$  (**2**). The photoreaction proceeds only in the presence of an O-atom acceptor (e.g.,  $\text{PPh}_3$ ) or in a solvent with reactive C–H bonds (e.g., THF and toluene; BDE  $\sim$  90 kcal/mol). By contrast, in benzene (C–H BDE  $>$  100 kcal/mol) no photoreaction occurs. The photoreduction of

(39) Rodriguez, R. E.; Kelly, H. C. *Inorg. Chem.* **1989**, *28*, 589–593.

(40) Maldotti, A.; Andreotti, L.; Molinari, A.; Carassiti, V. *J. Biol. Inorg. Chem.* **1999**, *4*, 154–161.

$[(^6\text{L})\text{Fe}^{\text{III}}-\text{O}-\text{Fe}^{\text{III}}-\text{Cl}]^+$  (**1**) is the first  $\mu$ -oxo bridged (heme) $\text{Fe}^{\text{III}}-\text{O}-\text{Fe}^{\text{III}}$ (non-heme) complex to demonstrate photochemically initiated oxygen atom transfer (OAT) chemistry of a similar nature to the heme-only systems. Analysis of the organic reaction products revealed a quantitative O-atom transfer to triphenylphosphine (to give  $\text{O}=\text{PPh}_3$ ), and multiple turnovers were possible with dioxygen present, suggesting photocatalysis and  $\text{O}_2$  reoxidation of **2** to **1**. In the case of photolysis reactions performed in solvents with weak C–H bonds, we suggest that homolytic C–H bond cleavage occurs via a photochemically generated Fe–oxo intermediate, as suggested in transient absorption laser photolysis studies. Organic radical species further react with dioxygen derived from workup leading to the observed carbonyl products. In the case of photolysis carried out under a dioxygen atmosphere, it is possible to achieve multiple product turnovers from THF to  $\gamma$ -butyrolactone and from toluene to benzaldehyde, suggesting a photocatalytic mechanism involving dioxygen as an oxidant.

Aromatic chlorocarbons are a class of persistent environmental pollutant, and much effort has been expended toward remediation of these compounds using inorganic coordination compounds. We discovered that a reactive species, photo-generated from  $[(^6\text{L})\text{Fe}^{\text{III}}-\text{O}-\text{Fe}^{\text{III}}-\text{Cl}]^+$  (**1**), was capable of aromatic C–Cl bond cleavage. The “additional” chloride ligands in the complex  $\{[(^6\text{L})\text{Fe}^{\text{III}}-\text{Cl}\cdots\text{Fe}^{\text{III}}-\text{Cl}]_2\text{O}\}^{2+}$  (**3**), relative to the starting material  $[(^6\text{L})\text{Fe}^{\text{III}}-\text{O}-\text{Fe}^{\text{III}}-\text{Cl}]^+$  (**1**), are derived from solvent (dichlorobenzene, chlorobenzene) or substrate (benzyl chloride) dechlorination. The reactions were found to proceed under both aerobic and anaerobic conditions, suggesting that the rapid build-up of a terminal (P) $\text{Fe}^{\text{III}}-\text{Cl}$  chloride species serves to block the (re)formation

of the parent  $[(^6\text{L})\text{Fe}^{\text{III}}-\text{O}-\text{Fe}^{\text{III}}-\text{Cl}]^+$  (**1**). The isolated metallo-complex  $\{[(^6\text{L})\text{Fe}^{\text{III}}-\text{Cl}\cdots\text{Fe}^{\text{III}}-\text{Cl}]_2\text{O}\}^{2+}$  (**3**) is a tetraferic species with a  $\mu$ -oxo non-heme diiron bridge. The observed organic reaction products from photolysis reactions performed in 1,2-dichlorobenzene and chlorobenzene included biphenyl trichlorides and biphenyl monochlorides, respectively. By contrast, the photolysis of  $[(^6\text{L})\text{Fe}^{\text{III}}-\text{O}-\text{Fe}^{\text{III}}-\text{Cl}]^+$  (**1**) in benzene/benzyl chloride resulted in the formation of  $\{[(^6\text{L})\text{Fe}^{\text{III}}-\text{Cl}\cdots\text{Fe}^{\text{III}}-\text{Cl}]_2\text{O}\}^{2+}$  (**3**) and benzaldehyde. The source of the oxygen atom in the product benzaldehyde is likely derived from dioxygen in the ambient atmosphere. Further investigations will be carried out to explore the scope and utility of  $[(^6\text{L})\text{Fe}^{\text{III}}-\text{O}-\text{Fe}^{\text{III}}-\text{Cl}]^+$  (**1**) or new analogues as a photoreagent or photocatalyst for the degradation of environmentally relevant chlorocarbons and other organic substrates.

**Acknowledgment.** This work was supported by the National Institutes of Health (Grant GM60353 to K.D.K.), the National Science Foundation (Grant CHE-9708222 to G.J.M.), and an NSF environmental research grant (CRAEMS, K.D.K. and G.J.M.).

**Supporting Information Available:** UV–vis spectra for the anaerobic photoreduction of **1** to **2** in benzene/ $\text{PPh}_3$  (Figure S1) and in toluene (Figure S2), mass spectral data for the organic dehalogenation products derived from photoreaction of **1** in 1,2-dichlorobenzene (Figure S3) and chlorobenzene (Figure S4), and spectral data for compound **3** including ESI-MS (Figure S5) and  $^1\text{H}$  NMR spectra (Figures S6 and S7). This material is available free of charge via the Internet at <http://pubs.acs.org>.

IC0490932